

# Chapter 2

## Neuronal Response Properties and Voltage-Gated Ion Channels in the Auditory System

Nace L. Golding

### 1 Introduction

One of the central challenges to auditory neuroscience is to understand how sound information is processed and transformed as it ascends to different levels in the brain. One way that the central auditory system is distinct from other sensory areas of the brain is the extent to which sound information is segregated at the earliest subcortical areas into different ascending pathways encoding different aspects of sound. For example, in the visual system, the first stage of information processing in the brain takes place in the lateral geniculate nucleus of the thalamus before proceeding directly to the primary visual cortex, where many of the major transformations in visual receptive fields occur. In olfaction, although extensive processing occurs in the olfactory bulb prior to the cortex, it is not apparent that there are topographic differences in how olfactory information is processed.

The aim of this chapter is to review how the coding of auditory information in different ascending pathways is influenced by synaptic integration, the process by which excitatory and inhibitory inputs sum together and trigger patterns of action potentials that reflect salient features of sounds. It will be made clear in this chapter that synaptic integration is strongly influenced, and in some cases dominated, by interactions between synaptic inputs and different classes of voltage-gated ion channels. Although mammalian systems are the primary focus, work from the avian auditory system will be discussed in specific instances. Particular attention will be on neurons of the cochlear nucleus and superior olivary complex, where the role of

---

N.L. Golding (✉)

Section of Neurobiology, Institute for Neuroscience, and Center for Perceptual Systems,  
University of Texas at Austin, Austin, TX 78712-0248, USA  
e-mail: golding@mail.utexas.edu

voltage-gated ion channels can be more easily understood within the context of well-defined circuit computations and functional roles. Two broad classes of neurons emerge: those with electrical properties that precisely maintain the temporal features encoded in their auditory inputs and those with electrical properties that transform synaptic input patterns into new patterns.

## **2 The Spatial and Temporal Structure of Auditory Input to the Brain**

In order to understand the nature of different auditory neurons' responses to sound stimuli, it is important to review two fundamental concepts in auditory neuroscience: tonotopy and phase locking. Sounds of different frequencies vibrate the basilar membrane of the cochlea in a topographic manner, with low frequencies vibrating more apical locations and high frequencies vibrating more basal locations. These vibrations are transduced into graded electrical signals by the cochlear hair cells, which in turn trigger patterns of action potentials in the spiral ganglion neurons (Nicolson, Chap. 3). Because neurons in the spiral ganglion innervate a limited number of hair cells, each ganglion cell carries information about a limited range of frequencies. Deflections of the stereocilia embedded in the basilar membrane cause a depolarization that leads to activation of voltage-gated calcium channels, causing calcium influx and the release of the excitatory neurotransmitter glutamate onto the endings of the spiral ganglion neurons. The activity of hair cells is converted into trains of action potentials by the spiral ganglion cells whose axons project to the brain via the eighth cranial, or auditory, nerve. All auditory information to the brain is carried by the auditory nerve fibers, which in turn synapse onto diverse cell targets in the cochlear nucleus, the first and obligatory integrative station in the brain. The cochlear nucleus possesses at least six classes of projecting neurons. Each of these pathways conveys different kinds of information, despite the fact that the pre-synaptic pattern of action potentials to these neurons is the same. There is an orderly representation of frequencies imposed by the paths of these auditory afferents in the brain. Their parallel orientation to one another in the cochlear nucleus creates a series of "iso-frequency" slabs, imposing frequency selectivity on the different cell types present in the cochlear nucleus. This organization is maintained through the projection patterns of neurons in the cochlear nucleus, thus creating tonotopic maps at successively higher levels in the auditory pathway.

Auditory afferents also convey critical information about sounds due to their ability to precisely represent periodic information in the patterns of their action potential output. This is commonly referred to as temporal coding. In hair cells, timed neurotransmitter release is brought about by the fact that hair cell signaling is directionally selective, with positive deflections of the stereocilia (toward the tallest stereocilia) triggering membrane depolarization and negative deflections resulting in membrane hyperpolarization. Thus, during acoustic deflections of the basilar membrane, hair

cells respond with cyclical depolarizing and hyperpolarizing voltage changes that reflect the frequency content of the stimulus. The corresponding cyclical release of neurotransmitter onto spiral ganglion cells imposes a restricted interval over which firing occurs, a phenomenon known as phase locking. In auditory nerve fibers, the axons of spiral ganglion neurons, phase locking occurs at frequencies generally below 2–4 kHz in mammals but extends up to 9 kHz in barn owls (Johnson 1980; Köppl 1997; Taberner and Liberman 2005). It is important to note that the precise phase locking of an individual auditory neuron does not require perfect one-for-one firing with each cycle of the acoustic stimulus. As many neurons encode a given frequency, the interval of the stimulus is encoded by the overall firing responses of the neural population as a whole.

### **3 Synaptic and Voltage-Gated Ion Channel Properties for Precise Temporal Coding**

Given the importance of timing information in the auditory system, a major focus of this chapter is on how interactions between synaptic inputs and voltage-gated ion channels maintain, and in some cases improve, the precision of the firing of action potentials. Some of the most intensely studied circuits that utilize timing information are introduced here.

#### ***3.1 Circuits That Utilize Timing Information***

##### **3.1.1 Coincidence Detection Across Frequencies in Octopus Cells of the Ventral Cochlear Nucleus**

Octopus cells are located in a distinct area of the posteroventral cochlear nucleus called the octopus cell area (Osen 1969). Their axons form a major ascending projection, giving rise to large calyceal endings in the contralateral ventral nucleus of the lateral lemniscus as well as the superior paraolivary nuclei (reviewed in Oertel 1999). These neurons are named after their distinctive dendritic architecture, which consists of large-caliber dendrites emanating from one pole of the soma. Octopus cells exhibit a distinct orientation with respect to the paths of the auditory nerve fibers, which provide their primary excitation. The cell body tends to be oriented toward the posterior octopus cell area, which receives inputs from lower-frequency afferents, and the dendrites extend roughly perpendicularly to the paths of the auditory nerve fibers toward higher-frequency regions (Fig. 2.1a) (Osen 1969; Kane 1973). Accordingly, octopus cells in vivo exhibit broad tuning curves and are effectively driven by transient broadband stimuli such as clicks (Godfrey et al. 1975;

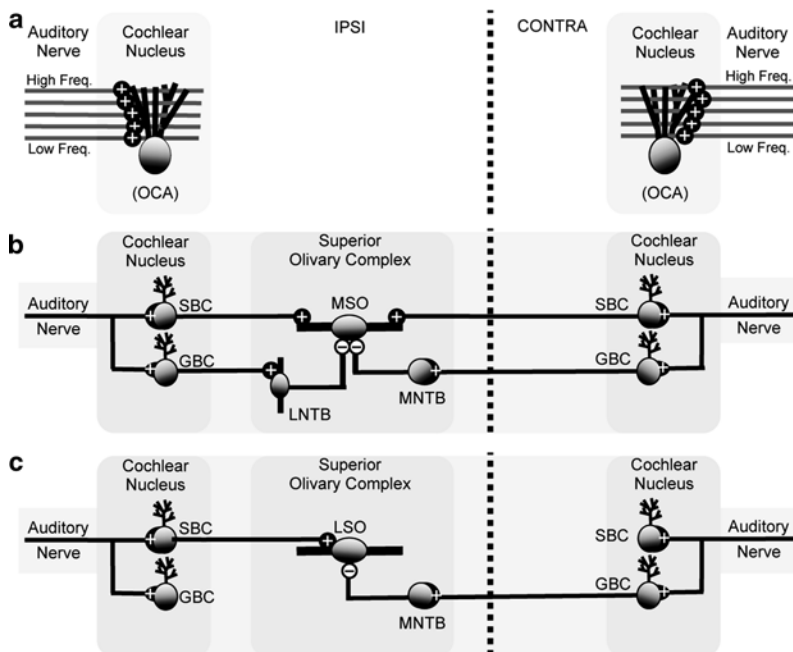


**Fig. 2.1** Three time-coding pathways in the auditory brainstem. (a) Octopus cells are clustered in a distinctive area of the posteroventral cochlear nucleus, the octopus cell area (OCA). Excitatory, glutamatergic inputs from auditory nerve fibers are organized tonotopically, with low-frequency fibers forming synapses on more proximal dendrites and higher-frequency fibers contacting progressively more distal dendrites. (b) Excitatory synaptic coincidence detection of binaural inputs in the medial superior olive (MSO). MSO principal neurons present in the superior olivary complex receive glutamatergic excitation from both ipsilateral and contralateral spherical bushy cells (SBCs) in the anteroventral cochlear nucleus, which in turn are driven by large calyceal synapses of auditory nerve fibers, the endbulbs of Held. MSO neurons are driven by two feedforward inhibitory nuclei, the medial and lateral nuclei of the trapezoid body (MNTB and LNTB). Both neuron types are primarily glycinergic and are driven by excitation from globular bushy cells (GBCs) of the posteroventral cochlear nucleus. Glycinergic inhibition in MSO principal neurons is targeted to the soma and proximal dendrites, whereas excitation is primarily dendritic and segregated to one side of a bipolar arbor. (c) Binaural processing in the lateral superior olive (LSO). LSO principal neurons receive ipsilateral excitation from ipsilateral spherical bushy cells and contralateral inhibition from MNTB principal cells. Similar to MSO principal neurons, LSO principal neurons receive somatic/proximal dendritic inhibition and dendritic excitation within a bipolar dendritic structure

Rhode and Smith 1986; Oertel et al. 2000). In response to tones and noise stimuli, octopus cells respond with an “onset” firing pattern, with a single well-timed spike followed by nearly no subsequent firing for the duration of the sound stimulus. Octopus cells likely integrate the convergence of at least 50 auditory nerve fibers (Golding et al. 1995). Because each input contributes only a small submillivolt depolarization to octopus cells’ postsynaptic responses, the initiation of action potentials requires strong synchronous activation of many auditory nerve fibers

tuned to a broad range of frequencies. In this way, octopus cell dendrites detect the coincident activity of a large population of auditory nerve fibers encoding a broad range of frequencies.

### **3.1.2 Computation of Interaural Time Differences in the Medial Superior Olive**

Neurons of the medial superior olive (MSO) are one of the major cell groups in the superior olivary complex and will be described, along with their avian homologs, in Chap. 6 by McLeod and Carr. The MSO is one of the first sites for integrating auditory activity from the two ears. MSO neurons are innervated by the spherical bushy cells that reside in the ipsilateral and contralateral ventral cochlear nucleus (Fig. 2.1b) (Cant and Casseday 1986; Smith et al. 1993; Beckius et al. 1999). Spherical bushy cells themselves are driven by only a few (1–3) powerful specialized endings from the auditory nerve, the endbulbs of Held (Manis et al., Chap. 4). The spherical bushy cells then provide conventional bouton-type excitatory synapses to MSO principal cells. The dendritic architecture of MSO principal cells is bipolar, with ipsilateral bushy cell input segregated to the lateral dendrites and contralateral bushy cells inputs restricted to the medial dendrites (Stotler 1953; Lindsey 1975). MSO neuron responses are also shaped by two feed-forward inhibitory nuclei, the medial and lateral nucleus of the trapezoid body (MNTB and LNTB, respectively). The principal neurons of the MNTB and LNTB are driven by contralateral and ipsilateral globular bushy cells in the cochlear nucleus, respectively (Borst and Rusu, Chap. 5).

As low-frequency sound sources move along the horizontal plane, the relative timing of bushy cell inputs to the superior olivary complex changes systematically, thereby changing the relative timing of excitatory and inhibitory inputs to MSO neurons. MSO neurons respond to these synaptic alterations by changing their rate of action potential firing. This activity is conveyed via the axonal projections of MSO neurons to the central nucleus of the inferior colliculus (Henkel and Spangler 1983; Nordeen et al. 1983; Loftus et al. 2004). In this way, MSO neurons detect the relative coincidence of synaptic inputs driven by the two ears and translate these differences into a rate code. Ultimately, this activity is utilized for the localization of sounds along the horizontal plane. Thus, the temporal resolution of the detection of binaural coincidence in the MSO has a clear relationship to the spatial acuity of horizontal sound localization.

### **3.1.3 Computation of Interaural Level Difference in the Lateral Superior Olive**

Neurons in the lateral superior olive (LSO) comprise the second major integrative stage for processing binaural cues in the auditory brainstem. The principal neurons of the LSO vary their rate of action potential firing according to differences in the level of sound intensity between the two ears. These level differences are most acute

at high frequencies because these frequencies are more susceptible to the effects of head shadowing. Consistent with this role, the frequency representation in the population of LSO neurons appears biased toward high frequencies (Guinan et al. 1972; Tsuchitani 1977). The circuitry of the LSO contains many of the same components as that of the MSO: principal neurons of the LSO receive phase-locked excitatory activity from ipsilateral spherical bushy cells of the cochlear nucleus and inhibitory glycinergic inputs from the contralateral principal neurons of the MNTB (Fig. 2.1c). As in the MSO, timing is critical in the LSO. As sounds move along the horizontal plane, the relative timing and hence the balance between excitatory and inhibitory synaptic inputs is altered, systematically changing the rate at which action potentials are generated. Whereas MSO neurons detect correlations between binaural excitatory inputs, effective signaling by LSO principal neurons relies on decorrelations between excitation and inhibition. Despite the different nature of their respective circuit computations, the ability of both MSO and LSO principal neurons to signal changes in sound location relies on the temporal precision of presynaptic excitatory and inhibitory inputs, as well as precision in the postsynaptic neurons themselves.

### ***3.2 Glutamate Receptor Properties for Fast Synaptic Excitation in Time-Coding Auditory Neurons***

In order to encode the temporal structure of sounds, neurons in auditory pathways concerned with timing information must reduce the time window over which they integrate auditory information. An obvious specialization required for this to occur is a reduction in the time course of excitatory synaptic currents. In birds and mammals, auditory neurons encoding fine timing information exhibit excitatory currents mediated primarily by  $\alpha$ -amino-3-hydroxy-5-methyl-4-isoxazolepropionic acid (AMPA)-type glutamate receptors. These receptors are characterized by fast rise times and short durations (generally <0.2 and 0.5 ms, respectively, at 34°C) (Raman et al. 1994; Isaacson and Walmsley 1995; Gardner et al. 1999). These properties reflect the molecular composition of the receptors. In the cochlear nucleus, bushy cells express primarily GluR3 and GluR4 subunits and express GluR2 subunits in less abundance (Hunter et al. 1993; Wang et al. 1998b). Studies in cell expression systems and auditory neurons have shown that these subunits yield receptors with fast gating and high calcium permeability (Geiger et al. 1995; Otis et al. 1995). Although the molecular composition of AMPA receptors has not been as thoroughly studied in other auditory nuclei, EPSP responses reflecting fast AMPA receptor gating is seen as a repeated motif in neurons in auditory nuclei involved in temporal coding, including the ventral cochlear nucleus (bushy cells), superior olivary complex (principal neurons of the MSO, LSO, and MNTB), and the ventral nucleus of the lateral lemniscus.

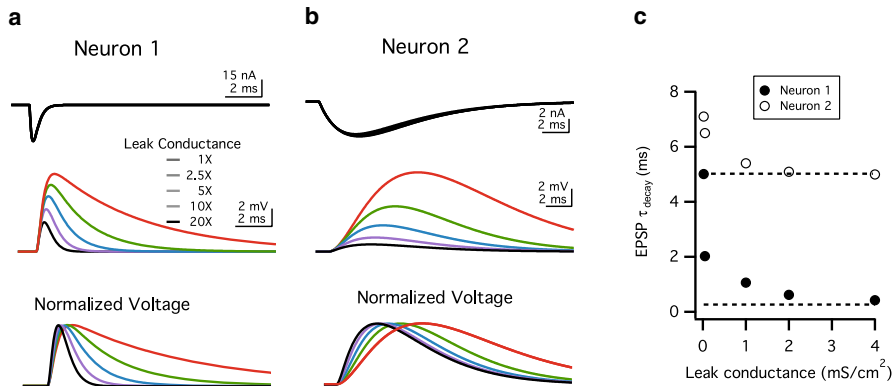


**Fig. 2.2** Effects of resting conductances on synaptic timing. Point-neuron models of a neuron exhibiting fast synaptic currents (**a**, “Neuron 1”) and synaptic currents 25-fold slower (**b**, “Neuron 2”). EPSCs and EPSPs (*upper* and *middle* traces, respectively) are shown for models exhibiting a 1- to 20-fold increase in membrane leak conductance. As membrane leak conductance increases (from 0.0002 to 0.004  $\text{S}/\text{cm}^2$ ), the amplitude and duration of EPSPs decrease in both models. In both cases, the time course of the EPSC is best reflected by models with the greatest leak conductance. However, EPSP duration in Neuron 2 is limited by the time course of the longer underlying synaptic current, whereas EPSP duration in Neuron 1 is sensitive to a larger range of leak conductance values. Synaptic conductances: 0.5 and 0.065  $\mu\text{S}$  for Neurons 1 and 2, respectively (**c**). Graphical representation of the decay time constant of the EPSP ( $\text{EPSP } \tau_{\text{decay}}$ ) as a function of membrane leak conductance for the examples in A and B. *Dotted lines* indicate the single-exponential time constant of decay for EPSCs in Neurons 1 and 2 (0.25 and 5 ms, respectively)

### 3.3 Resting Membrane Properties Establish the Time Course and Sensitivity of Synaptic Integration

#### 3.3.1 Contribution of Passive Leak Channels to Resting Membrane Properties

The fast kinetic properties of glutamate receptors would not translate into brief post-synaptic responses without corresponding specializations in the postsynaptic intrinsic membrane properties. Indeed, the speed of postsynaptic voltage responses is limited by the number of ion channels open at rest (which contributes to the membrane conductance). A simple illustration of this concept is shown in Fig. 2.2, which draws a comparison between two neurons with different integrative properties. The two model cells in this example have only a single compartment (i.e., soma only, no dendrites or axon) but Neuron 1 receives glutamatergic excitation that is 25 times faster than Neuron 2 (Fig. 2.2a, b, respectively). In these simulations, the number of leak channels is incrementally increased up to 20-fold from an initial value and the amplitude and time course of excitatory postsynaptic potentials (EPSPs) are

compared. In both neurons, the amplitude of EPSPs drops in proportion to the increased conductance according to Ohm's law:

$$\text{Ohm's law : } V_m = I_m / G_m \quad (2.1)$$

In Eq. 2.1,  $V_m$  is the membrane voltage,  $I_m$  is the synaptic current, and  $G_m$  is the resting membrane conductance. Note that while Ohm's law is most typically expressed in terms of membrane resistance (the inverse of membrane conductance), conductance is used here because of its direct and more intuitive relationship to ion channel expression. The speed of membrane voltage changes (quantified by the membrane time constant, or  $\tau_m$ ), is also inversely proportional to the membrane conductance, as:

$$\tau_m = C_m / G_m \quad (2.2)$$

In Eq. 2.2,  $C_m$  represents the membrane capacitance, which is proportional to the cell's surface area. Here the two model neurons differ in their responses: at the lowest membrane conductance level (1 $\times$ ), the response in Neuron 1 far exceeds the underlying synaptic current, because the slow membrane time constant limits the speed of the repolarization. As the resting leak conductance is increased, the time course of membrane repolarization more closely approaches the time course of the underlying synaptic current. In Neuron 2, the same effects are observed, but they are not nearly as dramatic because the longer time course of synaptic current imposes a lower limit on the time course of EPSPs. Thus, there are two important concepts illustrated by this simulation. First, there is a trade-off between membrane sensitivity and temporal precision, as increasing leak conductance simultaneously reduces voltage changes and the membrane time constant. Second, in order to encode synaptic timing information with precision, it is not sufficient for a neuron to exhibit neurotransmitter-gated receptors with rapid kinetics. The cell must also exhibit a resting conductance level that confers a membrane time constant low enough to avoid limiting the intrinsic time course of excitation.

At the molecular level, a family of genes has been identified and cloned that give rise to potassium leak currents. These are the so-called two-pore domain potassium channels, named after the two pore-forming loops in their predicted membrane topology. Of the eight family members that form functional channels and are expressed in the mammalian CNS, three (TASK-1, TASK-2, and TWIK-1) have been shown to be expressed in neurons of the cochlear nucleus (Talley et al. 2001; Berntson and Walmsley 2008). However, it is not yet known how these channel proteins are distributed in different cell types in auditory pathways. More recently, sodium-dependent leak channels have also been identified (NALCN, or "sodium leak channel, nonselective") (Lu et al. 2007). While this channel shows widespread distribution throughout the brain, its expression in auditory neurons has not yet been investigated. While leak channels are an important component of the passive membrane properties of all neurons, it will be seen that in many auditory neurons membrane properties may be dominated by voltage-gated ion channels active around the resting potential.



### 3.3.2 Contribution of Voltage-Gated Ion Channels to Resting Membrane Properties

While voltage-insensitive leak channels provide an important contribution to the passive electrical properties of neurons, there are few, if any neurons in the central nervous system that are purely passive. Along with leak channels, voltage-gated ion channels may also make important contributions to the resting properties of neurons, as long as they have a non-inactivating component of current that is active at the cell's resting potential. Two types of channels have been documented to be especially important: low voltage-activated (LVA) potassium channels, and the hyperpolarization and cyclic nucleotide-gated cation channels (HCN channels). Both channel types are discussed below.

#### Low Voltage-Activated Potassium Channels

A recurring channel motif in auditory brainstem neurons concerned with temporal coding is the presence of potassium currents that are activated at relatively hyperpolarized voltages. Current through these low voltage-activated potassium channels will be denoted as  $I_{K-LVA}$ , but in different studies this current has also been abbreviated as  $I_L$ ,  $I_{KLT}$ , and  $I_{KL}$ . The LVA potassium channels are expressed widely in many neurons in the brain and are often found enriched in the axon initial segment as well as in the nodes of Ranvier (Hopkins et al. 1994; Sheng et al. 1994; Kole et al. 2007). However, these channels are expressed in particularly high density in the cell bodies and dendrites of auditory brainstem neurons concerned with temporal coding (Manis and Marx 1991; Brew and Forsythe 1995; Bal and Oertel 2001). While there are differences in the details of the LVA potassium channel characteristics across different neuron types, they share several general features. First, the activation of these channels typically occurs at voltages slightly negative to the resting potential ( $\sim -65$  to  $-70$  mV), and given that LVA potassium channels have a non-inactivating component, the channels can provide a tonic conductance at rest. Second, LVA potassium channels across auditory neurons exhibit a similar pharmacological profile, being blocked by submillimolar concentrations of 4-aminopyridine as well as different fractions of dendrotoxin (dendrotoxin-I,  $\alpha$ -dendrotoxin, and dendrotoxin-K), a high-affinity toxin isolated from the African black or green mamba snake. Finally, LVA potassium channels exhibit fast (typically submillisecond) activation kinetics, allowing these channels to influence the timing, amplitude, and shape of subthreshold EPSPs and action potentials. These interactions will be discussed in Sect. 3.4.

The precise molecular composition of LVA potassium channels expressed in time-coding auditory neurons is not fully understood, but it is clear that they consist of members of the  $K_v$  subfamily (also referred to as Shaker-type potassium channels in *Drosophila*). Progress in understanding LVA potassium channel composition has been aided by the availability of toxins that target different  $K_v$  subunits with high specificity. LVA potassium currents in time-coding auditory neurons are consistently blocked by  $\alpha$ -dendrotoxin and dendrotoxin-I, toxins that block channels containing  $K_v1.1$ ,  $1.2$ , and  $1.6$  subunits (Brew and Forsythe 1995;

Ferragamo and Oertel 2002; Leão et al. 2006). Indeed, immunocytochemical and in situ hybridization studies indicate that the Kv1.1 subunit is expressed consistently in these areas, an observation supported by the extensive block of LVA potassium currents by dendrotoxin-K, which specifically targets potassium channels containing at least one K<sub>v</sub>1.1 alpha subunit in the tetramer (Bal and Oertel 2001; Dodson et al. 2002; Mathews et al. 2010). However, K<sub>v</sub>1 subunits can co-assemble with other members of the same family to form a functional channel (Hopkins et al. 1994), and several lines of evidence support the idea that LVA potassium channels are heteromeric combinations of different K<sub>v</sub>1 family subunits. For example, in principal neurons of the MNTB, LVA potassium currents have been subdivided into two approximately equal components based on their sensitivity to tityustoxin-K $\alpha$ , a blocker of K<sub>v</sub>1.2 subunits (Dodson et al. 2002). However, ~90% of the LVA potassium current is blocked by dendrotoxin-K, indicating that most channels contain K<sub>v</sub>1.1 subunits. These findings support the conclusion that LVA potassium channels in the MNTB consist of at least two classes of heteromeric channels, one containing K<sub>v</sub>1.1 and K<sub>v</sub>1.2 subunits, and the other containing K<sub>v</sub>1.1 and another K<sub>v</sub>1 family member, possibly K<sub>v</sub>1.6. Similarly, in octopus cells LVA potassium current is largely (~80%) dendrotoxin-K sensitive, but only about 50% of the LVA potassium current is blocked by tityustoxin-K $\alpha$  (Bal and Oertel 2001). The overall conclusion from these and other studies is that LVA potassium current is mediated by a heterogeneous population of channels containing different K<sub>v</sub>1 family subunits, with K<sub>v</sub>1.1 being present in the majority of channels.

What might be the functional consequences of having potassium channels comprised of different combinations of K<sub>v</sub>1 subunits? In expression systems, homomeric combinations of K<sub>v</sub>1.1 exhibit more negative activation ranges and faster kinetics than channels composed of only K<sub>v</sub>1.2 subunits, and heteromeric channels containing both subunits display intermediate properties (Hopkins et al. 1994). Thus the expression of channels with different subunit stoichiometry would provide a means for auditory neurons to, in a sense, “tune” channels to display the correct voltage sensitivity and kinetics in order to carry out specific computational roles. This is not the only way through which channel properties can be adjusted: channel kinetics and voltage-sensitivity can also be modified by the presence of accessory (nonpore-forming) subunits and neuromodulators. Thus at the molecular level there are multiple mechanisms by which channel properties can be modified, increasing the difficulty of interpreting differences in channel properties across different neuron types and even differences observed within the same neuron class.

### Hyperpolarization-Activated Cation Channels

HCN channels are comprised of a family of four gene products (HCN1–4). These channels are non-inactivating and typically have negative activation ranges that overlap to some extent with the resting potential. These features make HCN channels important determinants of the resting conductance of neurons, which in turn

influences the speed of membrane voltage changes, as discussed in Sect. 3.3.1. Thus, the degree to which these channels shape the resting conductance and membrane time constant depends critically on the density of channels, the voltage-dependence of activation, and the value of the resting potential. These factors vary widely across neuron types, even among time-coding auditory neurons. For example, octopus cells express HCN channels in high density ( $\sim 150$  nS whole-cell conductances), with 50% of the channels activated at  $-65$  mV. At the average resting potential of these cells of  $-60$  mV,  $I_h$  is a major determinant of the extraordinarily fast membrane time constant of these cells, which is  $\sim 200$   $\mu$ s (Golding et al. 1995; Bal and Oertel 2000). By contrast, bushy cells recorded under similar conditions exhibit lower whole-cell conductances ( $\sim 30$  nS), but perhaps more importantly the half-activation voltage for HCN channels is  $-83$  mV, possibly reflecting differences in subunit composition and/or modulatory state (Cao et al. 2007). As this value is far more negative relative to the resting potential of bushy cells, HCN channels make a relatively smaller contribution to the resting conductance, and the temporal precision found in these cells is more strongly influenced by other voltage-gated ion channels, particularly LVA potassium channels.

The interplay between HCN channels and LVA potassium channels deserves comment. The activation range of both channels overlaps in the voltage range near rest. Since the reversal potential of HCN channels typically resides between  $-20$  and  $-40$  mV, tonic activation of these channels near rest produces an inward current. By contrast, the reversal potential of LVA potassium currents is  $\sim -90$  mV, and thus activation of these channels at rest produces an outward current. When both channel types are expressed together in significant densities, the resting potential reflects the influence of both channels (Bal and Oertel 2000, 2001; Hassfurth et al. 2009). Each channel's activation moves the membrane potential away from its own activation range and toward that of the other. Thus the co-expression of HCN channels and LVA potassium channels comprises a homeostatic system that promotes the stability of the resting potential.

### ***3.4 Control of Synaptic Integration and Action Potential Timing by Low Voltage-Activated Potassium Channels***

The LVA potassium channels possess several properties that render them especially effective in controlling the timing of synaptic activity. First, as discussed in the previous section, LVA potassium channels typically activate at voltages similar or negative to the typical resting potentials of neurons (between  $-80$  and  $-60$  mV). Second, the activation of  $K_v1$  channels exhibits steep voltage dependence over the subthreshold voltage range (generally between  $\sim -65$  and  $-45$  mV). Third,  $K_v1$  channels exhibit activation kinetics that are fast enough to allow the channel to contribute to the repolarization of both subthreshold EPSPs and action potential waveforms.

### 3.4.1 Influence of Low Voltage-Activated Potassium Channels on Synaptic Potentials

In time-coding neurons of the auditory brainstem, the strength of the activation of  $K_v1$  potassium channels by EPSPs depends strongly on the rate of rise of excitation. Differences in rise time can arise in several ways. First, in neurons that integrate excitation from many inputs, a slower depolarizing envelope would be produced by acoustic stimuli that generate lower synchrony in presynaptic inputs. Second, concurrent inhibition also has the potential to shape the overall rate of rise of the depolarization. A striking demonstration of this concept comes from the octopus cells of the cochlear nucleus (Ferragamo and Oertel 2002). These authors observed that in octopus cells action potential initiation did not exhibit an absolute voltage threshold, but rather one that was highly dependent on the rate of rise of excitation. Indeed, spike initiation required a slope of greater than 12 mV/ms: with slower rising depolarizations, spikes could not be generated at any stimulus amplitude. The explanation for this result has to do with the interplay between  $K_v1$  channel kinetics and the rising phase of excitation. With sharply rising EPSPs, peak excitation is reached prior to strong activation of LVA potassium channels, allowing for the regenerative activation of sodium channels and the initiation of spikes to occur prior to strong activation of outward potassium current. With increasingly slower events, sodium channel activation is less synchronous and more extensively overlaps with the activation of potassium current, thus giving rise to ratios of inward to outward current that are increasingly less favorable for action potential initiation. In this way,  $K_v1$  channels narrow the time window over which synaptic inputs may sum effectively to produce action potential signaling.

Another way of thinking about the effects of  $K_v1$  channels on synaptic integration is as a high-pass filter that attenuates more slowly rising EPSPs. In MSO principal neurons, where action potential generation requires the submillisecond coincidence of binaural synaptic inputs,  $K_v1$  channels have been shown to reduce the number of “false-positive” spikes generated from synaptic activity that is uncorrelated with the synaptic activity driven by the stimulus (Svirskis et al. 2002, 2004).

In MSO principal neurons, excitation is targeted to the dendrites and then propagates “forward” to the soma and axon. This introduces a potential complication for temporal coding, as synapses located at different dendritic locations would be subject to variable degrees of electrotonic cable filtering. Cable filtering arises from the combined resistive and capacitive properties of the dendritic membrane, the effect of which is to delay the rise time of EPSPs, prolong their duration, and attenuate their amplitude. (Mathews et al. 2010) used paired somatic and dendritic recordings as well as modeling to examine how LVA potassium channels shape dendritic EPSPs as they propagate along the dendrites (Fig. 2.3). They found that while EPSPs undergo strong attenuation in their propagation to the soma, as would be expected, EPSPs become narrower in duration at the same time (Fig. 2.3a, b). This effect is due to the activation of dendrotoxin-sensitive  $K_v1$  channels, which are expressed at highest density in the perisomatic region of the cell, providing strong active repolarization of EPSPs, particularly near firing threshold. Based on this

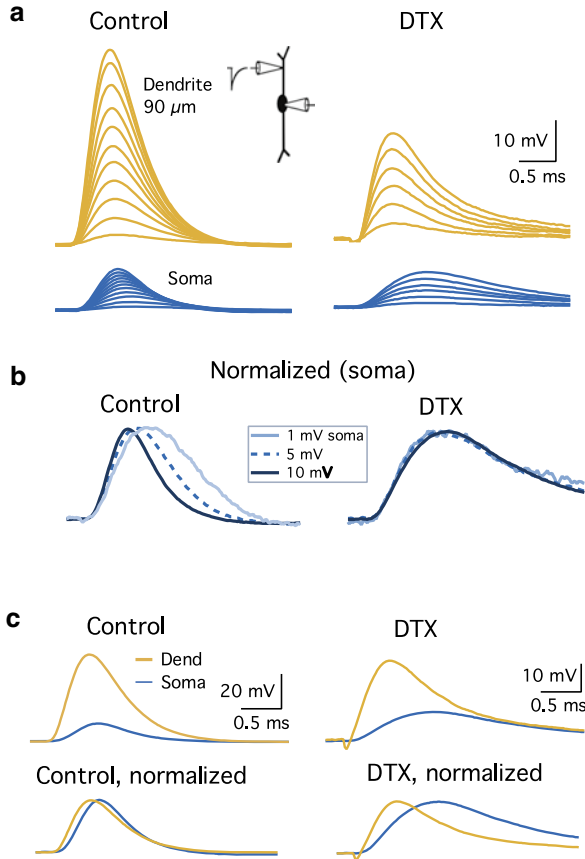


**Fig. 2.3** EPSP sharpening by  $K_v1$  channels. (a) Dual current-clamp recording from an MSO principal neuron from the soma and lateral dendrite 90  $\mu\text{m}$  away. Responses are shown to a family of simulated EPSCs (sEPSCs) injected into the dendrite. sEPSPs traversing the entire subthreshold voltage were recorded in physiological saline (*left traces*; 0.2–2.2, 0.2 nA step) and also in the presence of 100 nM  $\alpha$ -dendrotoxin (DTX), a blocker of  $K_v1$  potassium channels (*right traces*; 0.2–1.2, 0.2 nA step). (b) Normalized sEPSPs from three selected traces from the somatic recording show that larger voltage responses narrowed by  $\sim 40\%$  at 10 mV relative to 1 mV. This voltage-dependent sharpening was blocked in the presence of DTX. (c) The largest subthreshold sEPSPs show that cable distortions in EPSP rise time and duration as the sEPSP propagated from the dendrite to the soma were greatly enhanced when  $K_v1$  channels were blocked by DTX (Figure modified from (Mathews et al. 2010). With permission)

data, computational modeling of MSO principal neurons demonstrated that LVA potassium channels act as a high-pass filter. The stronger the broadening of EPSPs during dendritic propagation, the more robust the truncation of EPSPs by potassium channel activation. In this way, LVA potassium channels impose a relatively uniform duration for EPSPs arising from different dendritic regions, allowing EPSPs to more accurately reflect the relative timing of sounds to the two ears.

### 3.4.2 Effects of Low Voltage-Activated Potassium Channels on Action Potentials

Given the rapid activation of LVA potassium channels, it might also be expected that these channels influence the action potential waveform. This has been examined closely in the principal neurons of the MNTB, which fire trains of brief action potentials with high temporal fidelity at rates of up to ~600–800 Hz in vitro and in vivo (Taschenberger and von Gersdorff 2000; McLaughlin et al. 2008; Lortie et al. 2009). Analyses of  $I_{K-LVA}$  in MNTB neurons have shown that  $K_v1$ -containing LVA potassium channels are indeed activated during the course of the action potential, narrowing the action potential by up to ~40%, as well as increasing the depth of the spike afterhyperpolarization (Brew and Forsythe 1995; Klug and Trussell 2006). The large afterhyperpolarization in turn improves temporal coding by preventing multiple spikes from firing in response to a single synaptic volley (Fig. 2.4a), thereby reducing the variability in the timing of action potentials (Dodson et al. 2002; Gittelmann and Tempel 2006; Klug and Trussell 2006). These results are in accord with the increase in action potential jitter observed in MNTB recordings in vivo from  $K_v1.1$  knockout mice (Kopp-Scheinflug et al. 2003). While different  $K_v1$  channel subtypes are found to be localized to the soma, these channels also appear to be present in high density in the initial segment of the axon (Dodson et al. 2002), and are thus in a position to provide tight control over the threshold and timing of action potentials near their presumed site of initiation.

In octopus cells and MSO principal neurons, LVA potassium channels strongly regulate not only the shape of the action potential, but its amplitude as well. In these neurons, somatic action potentials appear unusually small (~5–20 mV). Blockade of LVA potassium channels results in roughly a threefold increase in action potential amplitude at the soma (Ferragamo and Oertel 2002; Scott et al. 2005) and improves the efficacy with which the larger action potential invades the distal dendrites (Scott et al. 2010) (Fig. 2.4b). Thus, in MSO principal neurons and octopus cells, an additional role for LVA potassium channels is to restrict access of the action potential to the soma and dendrites. Scott et al. (2007) have hypothesized that minimizing the amplitude of the action potential in the soma and dendrites might improve the temporal fidelity of synaptic integration by reducing the influence of the spike afterhyperpolarization on future cycles of synaptic integration during high-frequency synaptic input.

## 3.5 Control of Action Potential Signaling by High Voltage-Activated Potassium Channels

In addition to LVA potassium channels, many neurons contain potassium channels activated at voltages more positive to -30 mV, the high voltage-activated (HVA) potassium channels. A substantial proportion of these channels are typically blocked by millimolar concentrations of tetraethyl ammonium (TEA), but in many cases the molecular identity of the channel subunit configuration remains poorly defined. Members of the  $K_v3$  family of voltage-gated potassium channels have been shown to

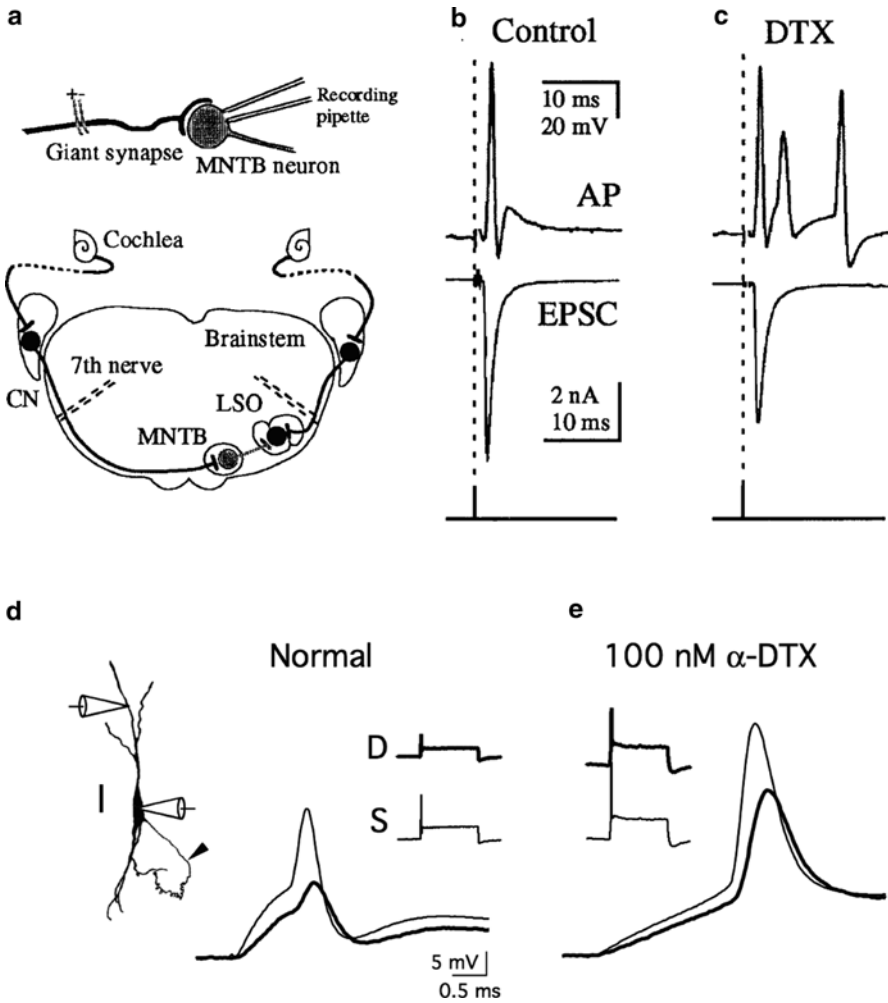


**Fig. 2.4** Influence of low voltage-activated potassium channels on action potential firing and backpropagation. Response of an MNTB principal neuron to presynaptic stimulation of the calyx of Held. (a) Experimental configuration. (Modified from Brew and Forsythe 1995, Figs. 1 and 7). (b) Under control conditions, calyceal stimulation evoked a single well-timed postsynaptic action potential. (Modified from Scott et al. 2007, Fig. 4. With permission). (c) However, when  $K_v1$  channels were blocked by 100 nM dendrotoxin-I, calyceal stimulation triggered repetitive firing. (d) Dual patch recordings from an MSO principal neuron from the soma (*thin traces*) and dendrite (*thick traces*; 75  $\mu$ m dendritic distance). A 1.6-nA somatic current pulse elicited transient firing (inset). In normal saline, the relatively small action potential was observed first at the soma and then at the dendrite, showing strong amplitude attenuation at the latter site. Anatomical scale bar: 20  $\mu$ m. Blockade of  $K_v1$  channels with 100  $\mu$ M  $\alpha$ -dendrotoxin (DTX) increased action potential amplitude threefold and strongly reduced the relative attenuation of the spike between the soma and dendrite. Current pulse 0.4 nA

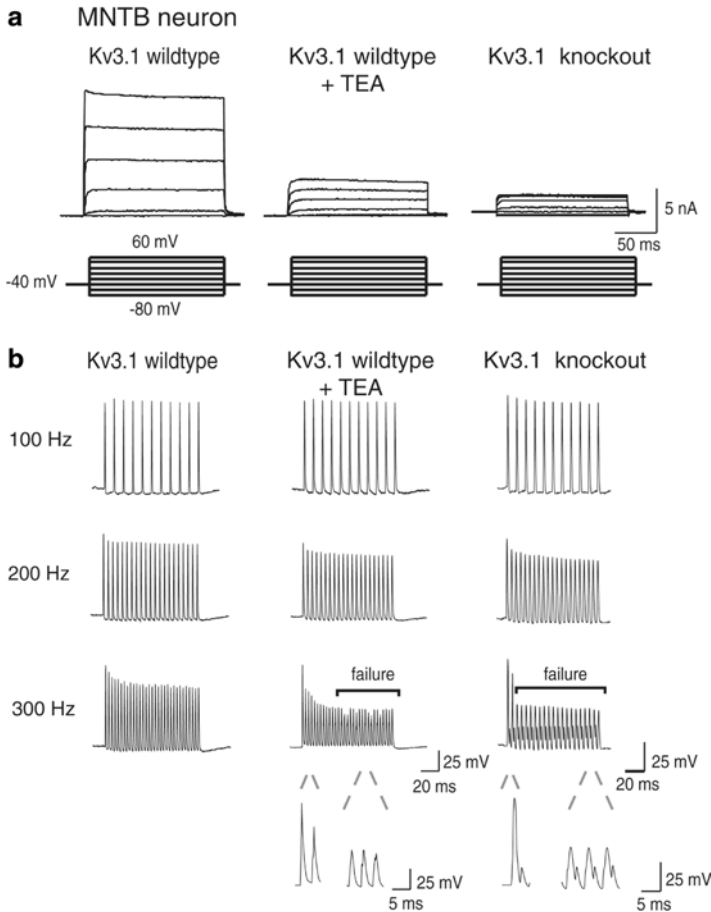


**Fig. 2.5** Role of  $K_v3.1$  potassium channels in high-frequency firing in MNTB principal neurons. **(a)** Whole-cell voltage clamp recordings of outward potassium currents in mouse MNTB neurons. Left: A family of potassium currents in an MNTB neuron from a wildtype mouse elicited by a family of voltage steps from  $-80$  to  $+60$  mV in  $10$  mV steps (left; “ $K_v3.1$  wildtype”). Middle: Currents were extensively blocked in the presence of  $1$  mM tetraethylammonium chloride (TEA). Right: Outward currents in MNTB neurons from  $K_v3.1$  knockout mice showed little high voltage-activated outward current, resembling the TEA condition from wildtype mice. **(b)** Action potential firing responses in current clamp under the same conditions as in A. Action potential failures were apparent at  $300$  Hz when  $K_v3.1$  currents were eliminated by TEA blockade or by genetic deletion in knockout mice (Figure taken from Macica et al. (2003) Fig. 1. With permission)

be expressed in several nuclei in the auditory pathway, including the cochlear nucleus, superior olive, and inferior colliculus (Perney et al. 1992; Perney and Kaczmarek 1997; Grigg et al. 2000). The expression of channels containing the  $K_v3.1$  subunit is particularly strong in the principal neurons of the MNTB. In these neurons, HVA potassium currents ( $I_{K-HVA}$ ) consist of a fast-activating current with little inactivation, a biophysical profile that bears high similarity to that exhibited by homomeric channels consisting of  $K_v3.1$  subunits (Fig. 2.5a) (Wang et al. 1998a; Macica et al. 2003).



While pharmacological block or genetic deletion of these channels has little effect on the ability of MNTB neurons to fire at frequencies lower than 200 Hz, at higher frequencies the absence of the channel leads to a greater incidence of action potential failures (Fig. 2.5b). An increase in action potential failures arising from a *reduction* in potassium current may seem counterintuitive, given that HVA potassium channels have been shown to narrow the width of MNTB spikes and increase the depth of spike afterhyperpolarizations (Klug and Trussell 2006). However, these results can be understood by considering how spike shape and repolarization influence voltage-gated sodium channels during repetitive firing. In the absence of  $I_{K-HVA}$ , an increase in the duration of the action potential will cause a larger population of voltage-gated sodium channels to inactivate, whereas the smaller afterhyperpolarization will reduce the proportion of voltage-gated sodium channels that can recover from inactivation. Thus, an essential function of  $I_{K-HVA}$  in MNTB neurons is to limit sodium channel inactivation by “resetting” the membrane potential to a relatively more hyperpolarized level.

### 3.6 Ion Channel Gradients Across Tonotopic Maps and Within Cells

#### 3.6.1 Potassium Channel Gradients Across Tonotopic Maps

Previous sections have described neurons in several time-coding auditory circuits as biophysically homogenous populations. However, there is a growing body of evidence indicating that in some auditory brainstem nuclei, the electrical properties of neurons vary according to tonotopic location. Just as the expression of different subtypes of voltage-gated ion channels critically influences the excitability of auditory neurons, differences in the expression levels of channels also strongly affect how neurons integrate synaptic information. Some of the best examples of these influences come from studies of time-coding principal neurons in the LSO and MNTB. Neurons in both the LSO and MNTB are arranged tonotopically, with low-frequency neurons positioned more laterally and high-frequency neurons located progressively more medially (Guinan et al. 1972; Tsuchitani 1977). In the LSO, Barnes-Davies and colleagues found that principal neurons could be divided into two electrophysiological types: transient-firing cells with relatively low input resistance ( $\sim 70 \text{ M}\Omega$ ) and repetitively firing cells with more than two times the input resistance of transient cells (Barnes-Davies et al. 2004). Furthermore, the distribution of these neurons varied according to tonotopic location, with transient-firing neurons more prevalent in lateral, low-frequency areas and repetitive-firing neurons in more medial, higher-frequency areas. The relative expression levels of dendrotoxin-sensitive LVA potassium channels play a key role in establishing this dichotomy. In voltage-clamp recordings, LVA potassium currents were significantly larger in transient versus repetitive-firing neurons, and in current-clamp recordings, blockade of these channels could convert transient firing neurons into repetitive-firing neurons. An idea presented by these authors is that the role of LVA potassium channels in preventing

multiple spikes per stimulus cycle is most important at acoustic frequencies below the phase-locking limit, where temporal precision is more relevant.

In the MNTB, the tonotopic expression pattern of HVA potassium channels appears reversed relative to that of LVA potassium channels in the LSO. Peak HVA potassium currents appear larger in more medial, high-frequency areas of the MNTB, in agreement with the relatively higher intensity of immunolabeled  $K_v3.1$  subunits in these regions (Li et al. 2001; von Hehn et al. 2004; Leão et al. 2006). Interestingly, similar findings have been observed in the avian cochlear nucleus and MSO (called the nucleus magnocellularis and laminaris, respectively) (Parameshwaran et al. 2001). Leão and colleagues have documented that MNTB principal neurons exhibit an increased ability to entrain to high-frequency depolarizations, consistent with the idea that  $K_v3$  channels improve high-frequency firing (Leão et al. 2006).

The modulatory state of  $K_v3.1$  channels also contributes to the functional gradient of  $K_v3.1$  currents in MNTB principal neurons. MNTB principal neurons express two splice variants of the  $K_v3.1$  gene,  $K_v3.1a$  and  $K_v3.1b$ . However,  $K_v3.1b$  is expressed more highly in mature neurons (Perney et al. 1992; Liu and Kaczmarek 1998). Only  $K_v3.1b$  is subject to phosphorylation by protein kinase C, which reduces current through the channel by decreasing its open probability (Macica et al. 2003). Song and colleagues have shown that quiescent MNTB neurons exhibit higher levels of phosphorylated  $K_v3.1b$ , but trains of synaptic stimulation *in vitro* or auditory activity *in vivo* dephosphorylate the channel, thereby increasing the amplitude of  $K_v3.1$  current. These activity-dependent changes in channel function ultimately improve the ability of MNTB neurons to follow higher-frequency stimuli, though apparently at the cost of temporal precision (Song et al. 2005). In slices, the ratio of dephosphorylated to phosphorylated  $K_v3.1b$  differs topographically, being higher in medial high-frequency regions.

While many questions remain regarding the nature and functional significance of potassium channel gradients in auditory nuclei, the preceding studies indicate that the expression of ion channels is not rigidly programmed within a cell type but has the capability of being fine-tuned to better respond to varying demands imposed by differing patterns of input activity. The mechanisms by which neurons achieve this tuning remain an important avenue of investigation.

### **3.6.2 Gradients of Voltage-Gated Potassium and Sodium Channel Gradients in the Dendrites of Single Cells**

Just as differential expression of voltage-gated ion channels affects the integrative properties of neurons located in tonotopic regions, recent findings in MSO principal neurons support the idea that ion channels can be nonuniformly expressed along the dendrites of individual neurons. In time-coding neurons of the MSO, both voltage-gated sodium channels and LVA potassium channels are expressed in higher density at the soma than in the dendrites (Mathews et al. 2010; Scott et al. 2010). The lack of strong sodium channel expression in MSO dendrites is a major factor underlying

the weak backpropagation of action potentials in these neurons (Scott et al. 2007). Electrophysiological mapping of the relative density of LVA potassium currents along MSO dendrites revealed that potassium channels are expressed in a gradient, with somatic channels expressed at an approximately fourfold higher density than in the distal half of the dendrites. As a result, LVA potassium currents are strongest at the soma and axon, close to the site of action potential initiation. As discussed in Sect. 3.4.1, this pattern of channel expression has been shown to be important for maintaining a uniform duration of EPSPs as they propagate along the dendrites to the soma and axon.

## 4 Circuits that Transform Action Potential Patterns: The Influence of Voltage-Gated Ion Channels

The previous sections of this chapter have focused on how different ion channels enable the precise encoding of the timing of presynaptic inputs. However, in many circuits of the auditory system neurons do not exhibit the kinds of synaptic and biophysical specializations that are prerequisites for fast temporal computations. Instead, the firing pattern of presynaptic inputs is transformed into new patterns. As is the case in most neurons, the type, density, and distribution of voltage-gated channels plays an integral part in generating these patterns.

### 4.1 *Chopping Responses in Neurons of the Ventral Cochlear Nucleus and Superior Olive*

Chopping refers to the repetitive firing behavior exhibited by certain auditory neurons in response to acoustic stimulation. A chopping response consists of a well-timed initial spike followed by a train of spikes generated at a regular interval that is unassociated with that of the acoustic stimulus (Fig. 2.6). Chopping responses can be found in many neurons at several different levels of the auditory system, including the dorsal and ventral cochlear nuclei, LSO, periolivary nuclei, and inferior colliculus (Tsuchitani 1977; Blackburn and Sachs 1989; Rees et al. 1997). However, chopping has been most extensively studied in the ventral cochlear nucleus, where two broad categories of chopping responses have been correlated with two different types of stellate cells (reviewed in Oertel et al. 2010). Sustained chopping responses (“C<sub>s</sub>” units in vivo) exhibit regular firing for the duration of the acoustic stimulus (Rhode et al. 1983; Young et al. 1988; Smith and Rhode 1989). These cells correspond to “T stellate cells,” multipolar neurons that provide excitatory input to several higher-order auditory nuclei (Oertel 1983; Smith and Rhode 1989; Oertel et al. 1990). Onset choppers (“O<sub>c</sub>” units in vivo) display broad frequency tuning, and in contrast to sustained choppers, they provide chopping responses only for a limited number of cycles during acoustic stimulation. Onset choppers have been associated

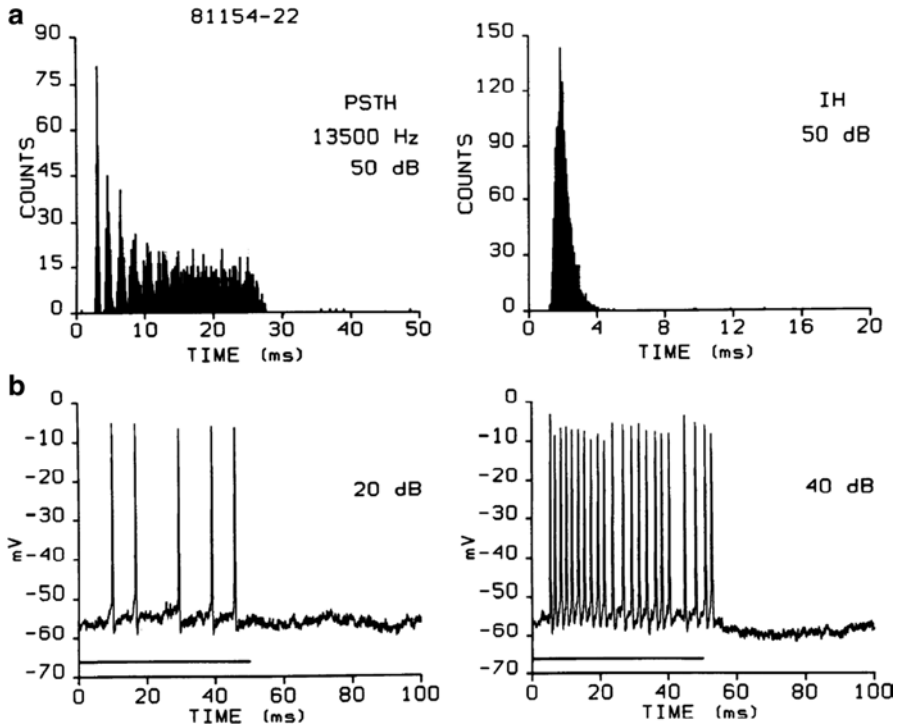


**Fig. 2.6** Extracellular and intracellular recording of chopping responses in presumed VCN stellate neurons in vivo. (a) Peristimulus time histogram (“PSTH,” left) showing the temporal response pattern of a VCN chopper unit in response to a 25-ms pure tone stimulus presented at the cell’s characteristic frequency of 13.5 kHz. The interspike interval histogram (“IH,” right) illustrates the cell’s preferential interspike interval over a narrow range of frequencies. (b) Intracellular records from the same cell in (a), showing action potential trains, with increased variability in spike timing apparent later in the response to the higher intensity stimulus (right) (Figure taken from Rhode and Smith 1986, Fig. 17. With permission)

with the “D stellate cells” (see Trussell, Chap. 7), which provide inhibitory input to targets in the ipsilateral dorsal cochlear nucleus and contralateral cochlear nuclei (Smith and Rhode 1989; Oertel et al. 1990; Doucet and Ryugo 1997).

Sustained firing in stellate cells requires appropriate properties of both synapses and voltage-gated ion channels. At synapses between auditory nerve fibers and stellate cells, excitation through AMPA-type glutamate receptors is fast and brief, similar to other auditory nerve synapses in the VCN (Gardner et al. 1999, 2001). However, T stellate cells express a relatively higher NMDA receptor density than other VCN neurons, which might broaden EPSPs at depolarized membrane potentials (Cao and Oertel 2010). The longer membrane time constant (on the order of milliseconds) of stellate cells combined with polysynaptic excitation from neighboring t-stellate cells (Ferragamo et al. 1998) improves the ability of these cells to maintain prolonged excitation throughout trains of synaptic stimuli.

In contrast to the time-coding neurons discussed in Sect. 3, in stellate cells the voltage-gated conductances that shape subthreshold synaptic responses are notably absent. Accordingly, blockade of voltage-gated potassium conductances in time-coding neurons often generates repetitive, chopping-like responses (Banks and Smith 1992; Barnes-Davies et al. 2004; Svirskis et al. 2002). While stellate cells do express HCN channels, the activation range of these channels is far more hyperpolarized than time-coding neurons such as octopus cells and principal neurons of the MSO and LSO, and thus HCN channels make only a small contribution to the resting potential and input resistance (Rodrigues 2005). In dissociated VCN cells presumed to be stellate cells, little or no LVA potassium current was recorded (Manis and Marx 1991). Together these results explain the highly linear voltage-current relationship that has been described in VCN stellate cells (Wu and Oertel 1984; Manis and Marx 1991; Rodrigues 2005). Such properties allow for extensive temporal summation of even weak excitatory synaptic inputs from the auditory nerve, an important aspect of maintaining sustained firing throughout the course of a stimulus.

The observation that chopping responses occur at an intrinsic frequency independent of the frequency of the acoustic stimulus highlights the critical role played by voltage-gated ion channels, particularly in regard to the repolarization of the action potential. Manis and Marx (1991) showed in dissociated VCN neurons that “type I” cells (presumed to be stellate cells) possessed two types of HVA potassium currents with similar voltage sensitivity. Both currents activated near  $-30$  mV but exhibited differing kinetics, with fast and slow activation time constants of  $\sim 1$  and  $13$  ms. These authors noted the importance of the slower component in controlling the interspike interval of firing, as cell-to-cell differences in the magnitude and kinetics of the slower component would be expected to influence the depth and rate of recovery from the spike afterhyperpolarization. They further proposed that the cell-to-cell variability in kinetics of the slow component might underlie in part the heterogeneity in chopping frequency and regularity that has been reported in single-unit recordings in vivo. While many factors can influence the frequency and regularity of chopping responses, including the number and dendritic location of excitatory and inhibitory synaptic inputs (Banks and Sachs 1991; Paolini et al. 2005), the strength and kinetics of action potential afterhyperpolarizations are important considerations. In studies of regular-firing neurons in the LSO in vitro, calcium-activated potassium channels have been shown to be a prominent component of the spike afterhyperpolarization (Adam et al. 2001), and modeling studies have predicted that these channels are likely to be important in establishing the frequency of chopping (Zackenhause et al. 1998; Zhou and Colburn 2010). Thus while the synaptic and ion channel mechanisms underlying chopping responses may differ across neuron types in different nuclei, regulation of the action potential afterhyperpolarization is undoubtedly a common factor that shapes chopping characteristics in many neuron types, even if there is diversity in the underlying ion channels.

## 4.2 The Influence of A-Type Potassium Channels on Pauser/Buildup Responses in Fusiform Cells of the Dorsal Cochlear Nucleus

Fusiform cells of the dorsal cochlear nucleus (DCN) receive direct excitation from auditory nerve fibers and provide the major excitatory output from the dorsal cochlear nucleus. In vivo, fusiform cells often generate a characteristic temporal response known as a “pauser/buildup” pattern, consisting of either a transient response followed by a ramped increase in firing rate or simply a ramped increase in firing in the absence of an initial transient response (i.e., a pause).

Fusiform cell responses are influenced by the interaction between synaptic responses and “A-type” potassium channels so-named from their original description in the marine gastropod *anisodoris* (Connor and Stevens 1971). The critical features of these channels include activation at voltages below action potential threshold and fast inactivation that occurs over a voltage range near and depolarized to the resting potential. Kanold and Manis (1999) showed that in DCN fusiform cells, one of two types of inactivating potassium currents fits this profile, which they termed  $I_{KIF}$  for “fast-inactivating potassium current.” In fusiform cells,  $I_{KIF}$  activates rapidly, with a time constant less than 1 ms, and inactivates on the order of ~11 ms (Kanold and Manis 1999). Since this A-current inactivates extensively in the voltage range near rest, its magnitude depends sharply on the electrophysiological context in which it is activated: A-current is large in magnitude when activated from negative voltages but almost completely absent when activated from a voltage range near or just above the typical resting potential of fusiform cells (Fig. 2.7a). It should be noted that while the A-current terminology is a useful functional description of currents found in many neurons from many types of organisms, at the molecular level A-current can be generated from alpha-subunits of different potassium channel subfamilies, most notably  $K_v1.4$  or  $K_v4.2$ . Fusiform cells have been shown to express the mRNA for  $K_v4.2$  channels (Fitzakerley et al. 2000), but the expression level of  $K_v1.4$  mRNA or protein is not known.

There are two important functional consequences of these channel characteristics for synaptic integration in fusiform cells. First, at membrane potentials just negative to rest, rapid activation of A-current by EPSPs transiently suppresses repetitive firing, inducing a “buildup” of firing rate with time. If strong enough, A-current can suppress initial firing entirely, generating a long “pause.” However, once activated, A-current inactivates over a time scale of tens of milliseconds, releasing the membrane from its hyperpolarizing influence and allowing repetitive firing to occur later during the course of the stimulus (Fig. 2.7b).

Fusiform cells have complex receptive fields that are strongly shaped by two broad types of inhibitory inputs: a fast frequency-specific input that exhibits similar tuning as excitation and a far more broadly tuned input (Young et al. 1992; Oertel and Young 2004). Because A-type potassium channels are sensitive to small changes in membrane potential near rest, the prediction is that the firing pattern of fusiform cells depends on both the level and duration of synaptic inhibition immediately prior

Synaptic Mechanisms in the Auditory System

Trussell, L.O.; Fay, R.R.; Popper, A.N. (Eds.)

2012, XIV, 234 p.,

ISBN: 978-1-4419-9517-9